THE JOURNAL OF PHYSICAL CHEMISTRY A

Article

pubs.acs.org/JPCA

# Metal Ion Complexes with HisGly: Comparison with PhePhe and PheGly

Robert C. Dunbar,*[,†] Jos Oomens,*[,‡,§] Giel Berden,[‡] Justin Kai-Chi Lau,[∥] Udo H. Verkerk,[∥] Alan C. Hopkinson,[∥] and K. W. Michael Siu*[,∥]

[†]Chemistry Department, Case Western Reserve University, Cleveland, Ohio 44106, United States

[‡]Radboud University Nijmegen, Institute for Molecules and Materials, FELIX Facility, Toernooiveld 7, 6525 ED Nijmegen, The Netherlands

[§]University of Amsterdam, Science Park 904, 1098XH Amsterdam, The Netherlands

[∥]Department of Chemistry and Centre for Research in Mass Spectrometry, York University, 4700 Keele Street, Toronto, Ontario, M3J 1P3, Canada

Supporting Information

**ABSTRACT:** Gas-phase complexes of five metal ions with the dipeptide HisGly have been characterized by DFT computations and by infrared multiple photon dissociation spectroscopy (IRMPD) using the free electron laser FELIX. Fine agreement is found in all five cases between the predicted IR spectral features of the lowest energy structures and the observed IRMPD spectra in the diagnostic region 1500−1800 $cm^{-1}$, and the agreement is largely satisfactory at longer wavelengths from 1000 to 1500 $cm^{-1}$. Weak-binding metal ions ($K^+$, $Ba^{2+}$, and $Ca^{2+}$) predominantly adopt the charge-solvated (CS) mode of chelation involving both carbonyl oxygens, an imidazole nitrogen of the histidine side chain, and possibly the amino nitrogen. Complexes with $Mg^{2+}$ and $Ni^{2+}$ are found to adopt iminol (Im) binding, involving the deprotonated amide nitrogen, with tetradentate chelation. This tetradentate coordination of Ni(II) is the preferred binding mode in the gas phase, against the expectation under condensed-phase conditions that such binding would be sterically unfavorable and overshadowed by other outcomes such as metal ion hydration and formation of dimeric complexes. The HisGly results are compared with corresponding results for the PheAla, PheGly, and PhePhe ligands, and parallel behavior is seen for the dipeptides with N-terminal Phe versus His residues. An exception is the different chelation pattern determined for PhePhe versus HisGly, reflecting the intercalation-type cation binding pocket of the PhePhe ligand. The complexes group into three well-defined spectroscopic patterns: nickel and magnesium, calcium and barium, and potassium. Factors leading to differentiation of these distinct spectroscopic categories are (1) differing propensities for choosing the iminol binding pattern, and (2) single versus double charge on the metal center. Nickel and magnesium ions show similar gas-phase binding behavior, contrasting with their quite different patterns of peptide interaction in condensed phases.

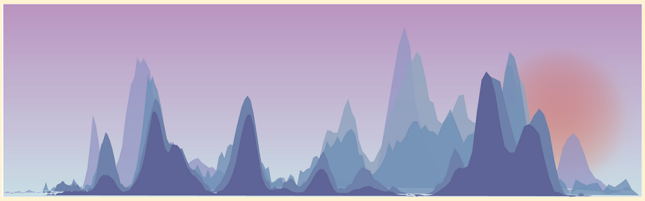

## INTRODUCTION

Incorporation of metal ions into peptide and protein molecules characteristically involves chelation of the metal ion at several Lewis basic sites drawn from both the amide linkages and the amino acid side chains. Histidine is one of the common side-chain-chelating residues in such structures, and it is interesting to explore the gas-phase (solvent-free) binding geometries for a model peptide giving possibilities of both amide backbone and also strong side-chain interactions with a bound metal ion.

Histidine has received extensive attention as a peptide residue active in metal ion binding, based on the affinity of the imidazole side chain for divalent metal ions. The imidazole nitrogen has been singled out as a particularly effective anchor point for metal ion chelation in peptide chains.[1−4] Studies of metal ion interactions including Co(II), Ni(II), and Cu(II) with HisGly and GlyHis in solution and in crystals have been frequent since at least the 1970s. Some aspects having continuing interest are oxygen binding and transport by metal ions such as Cu(II) in His-containing peptides,[5] the role of M(II) binding to His residues in prion proteins and their fragments,[6] and the subtle variations in the propensity of M(II) ions to deprotonate and bind to an amide nitrogen in competition with, or in concert with, binding to the imidazole nitrogen.[3] The literature is extensive: leading references can be found for instance in refs 3, 4, and 7−13.

Contrasting with the large body of solution-phase studies,[9] gas-phase investigation of metal ion binding to His-containing peptide model compounds has been sparse. Spectroscopic structure studies of metal ion complexes of the amino acid histidine[14−16] as well as the protonated amino acid,[17] anion

Received: March 4, 2013
Revised: May 24, 2013
Published: May 24, 2013

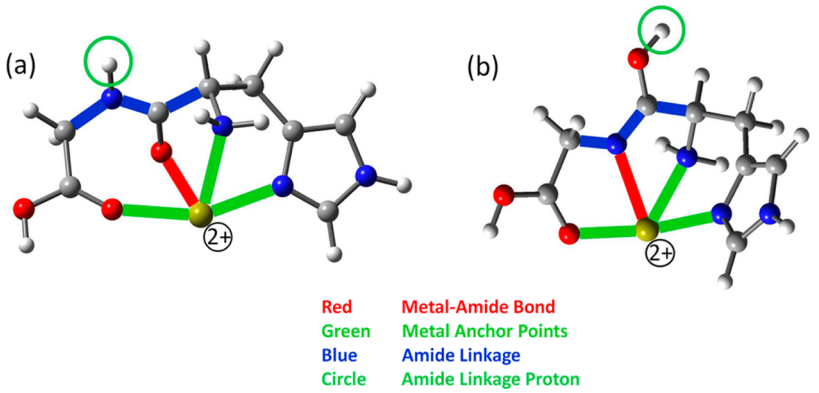


**Figure 1.** Metal ion binding site for HisGly. (a) Charge-solvated (CS) binding (CS $OONN_i$) to the amide carbonyl oxygen (red bond) along with Lewis basic anchor points (green). (b) Iminol binding (Im $ONNN_i$) to the deprotonated amide nitrogen, along with anchor points.

complexes,[18] and the radical cation[19] have been reported. Moreover, protonated AlaHis and HisArg have been examined spectroscopically.[20,21] Properties of some ionic and cationized forms of the amino acid have also been probed using nonspectroscopic gas-phase approaches.[22−25] However, gas-phase metal ion complexes of His-containing dipeptides have hardly been characterized. Kapota and Ohanessian[26] have studied the low-energy conformers of the sodium bound HisGly and GlyHis complexes computationally employing quantum chemical calculations.

As a ligand in metal ion complexes, the HisGly dipeptide, similar to the PhePhe dipeptide,[27] is notable for offering the metal ion multiple basic chelation sites, including the Lewis basic end groups of the peptide, the basic atoms of the amide linkage, and the basic sites presented by the histidine side chain. It is common in dipeptides for the ligand to chelate the metal ion by binding to a Lewis basic site on the central amide linkage, accompanied by stabilization by further chelation at anchor sites on the end groups and side chain. The first interesting question regarding this amide-based chelation architecture is whether the metal ion binds to the amide carbonyl oxygen, or instead displaces the proton on the amide nitrogen. In the latter case, which we shall refer to as the *iminol* binding motif, tautomerization of the peptide linkage occurs concurrently with binding of the metal ion to the amide nitrogen.[27] These two motifs are illustrated for the $Ca^{2+}$HisGly complex in Figure 1. Direct proof that both the carbonyl oxygen and the deprotonated nitrogen sites of a peptide amide linkage can simultaneously chelate a metal ion is currently lacking, although such binding has been suggested at least for model amide compounds with alkali metals.[28−30]

Complexation of HisGly by transition metal ions has been observed and characterized in solution,[11] notably with $Ni^{2+}$ [31] and $Cu^{2+}$.[32] For both of these metal ions at low pH (below 5 or 6), monomeric complexes are formed with charge-solvated (CS) type binding of the metal ion[32] (for copper, for example, this is the structure CS $O_aNN_i$ in our terminology, vide infra). At higher pH, deprotonation of the amide nitrogen occurs in the case of copper, giving a dimeric structure with deprotonated iminol-type binding of both copper ions. For the nickel complex, deprotonation of the amide nitrogen is not observed over the entire range of pH for which the monomer complex has been observed.

It has been considered that steric hindrance precludes the simultaneous binding of all three available nitrogen atoms (amino terminus, histidine side chain, and deprotonated amide) of HisGly or HisAla to Ni(II) in solution.[11,31,33] However, in the gas phase the strong driving force toward maximal coordination of the nickel center, along with the absence of alternative Lewis basic donor groups (such as water or a second peptide ligand), can lead to concurrent binding of all possible donor atoms on the HisGly ligand, and the HisGly chain is able to fold in a geometry making such coordination of all three nitrogen atoms favorable. Thus the monomeric four-coordinate iminol complexes of nickel and magnesium ions observed in the present study (vide infra) are uniquely gas-phase constructs in which the metal ion maximizes its intramolecular coordination in the presence of a single dipeptide ligand.

The new infrared-spectroscopic tool of infrared multiple photon dissociation spectroscopy (IRMPD), based on the combination of a powerful tunable infrared light source with a mass spectrometer, has the capability to characterize the in situ structures of mass selected gas-phase complexes.[34−46] Application of this approach in the mid-infrared wavelength region has been found to be particularly good at distinguishing the two different binding modes of interest here, and the free electron laser (FEL) light source coupled to a Fourier transform ion cyclotron resonance (FT-ICR) mass spectrometer at the FELIX facility has been brought to bear on the study of gas-phase metal ion−peptide complexes. The comparable facility at the CLIO FEL has engaged in similar studies. Some examples of the application of spectroscopic approaches to the study of dipeptide systems can be seen in refs 27, 36, 37, 42, 43, 47, and 48.

## METHODS

**Computation.** All the calculations were carried out using the Gaussian03 quantum chemical package.[49] For calculations of the HisGly complexes, extensive surveys of the potential energy surface were performed at the B3LYP/6-31G(d) level and the best structures were further optimized at the B3LYP/6-311++G(d,p) level.[50−56] For Ba the SDD basis set with a relativistic effective core potential was used.[57]

Density functional theory (DFT) calculations of the PhePhe complexes have been described previously.[37] However, PheAla calculations with most of these metal ions have not been reported. Here structure searches and vibrational calculations were carried out at the B3LYP/6-31+G(d,p) level at the LISA Linux cluster of the SARA Supercomputer center in Amsterdam. For comparison of DFT spectra to IRMPD spectra, the computed frequencies were scaled by a factor of 0.976, which is known to be adequate at the current levels of


dx.doi.org/10.1021/jp4021917 | J. Phys. Chem. A 2013, 117, 5335−5343

theory.[42] Computed spectra were convoluted with a 20 or 30 $cm^{-1}$ full width at half-maximum (fwhm) Gaussian line shape function for comparison to experimental IR spectra.

All of the calculated structures were L enantiomers of the residues (L-His and L-Phe residues). Kapota et al.[26] calculated the lowest energy conformation of neutral HisGly to be their $N^{\varepsilon}$ (I-1-a) structure, and we have referenced all the ion binding energies to this structure. The binding energy is the (negative of) the enthalpy of the complex minus the enthalpies of the neutral peptide and the bare metal cation. The Ni(II) complexes were calculated in the triplet state, since the singlet states of corresponding isomers are much higher in energy.

**IRMPD Experiments.** IR spectra of the gaseous metal ion−dipeptide complexes were recorded employing a Fourier transform ion cyclotron resonance mass spectrometer (FT-ICR MS) coupled to the Free Electron Laser for Infrared eXperiments (FELIX), as has been detailed elsewhere.[37,40] Metal ion−peptide complexes were generated by electrospray ionization (ESI, Waters Z-Spray) from a solution containing the peptide and metal salt in acetonitrile/$H_2O$ (~4:1). Target ions were trapped and mass selected in the FT-ICR cell and were irradiated with the wavelength-tunable infrared light from FELIX. Plotting the sum of all dissociation channels ratioed to the total ion count as a function of laser frequency, an infrared action spectrum was generated, and it was interpreted as a surrogate IR spectrum of the complex. To assign conformational and tautomeric structures, DFT computed linear IR spectra of candidate ion structures were compared with the observed spectra, where the calculated relative energetics provided additional guidance.

**Structure Labels.** The calculated conformers of the complexes are labeled in a straightforward way, such as "Im NOR", with the first letters indicating the character of the motif, being either charge solvated (CS), zwitterionic (ZW), or iminol (Im), and the remaining letters indicating all of the Lewis basic anchor points to which the metal ion is clearly bonded. (The caption of Figure 1 shows two examples.) The "$N_i$" symbol indicates a bond to an imidazole ring nitrogen of the His residue, and the letter "R" indicates a cation−$\pi$ interaction with a phenyl ring (for PheAla, PheGly, and PhePhe). In cases of ambiguity, the amino and imidazole nitrogens are distinguished by subscripts "a" and "i", respectively, and the carboxyl and amide carbonyl oxygens by "c" and "a". When a double-well OHN hydrogen bond occurs, the symbols "OH" or "NH" are appended to indicate the heavy atom to which the H is primarily bound. When a structure with CS-type binding of the metal ion undergoes a proton shift to become zwitterionic, a symbol (ZW) is appended to the end of the structure label.

## RESULTS AND DISCUSSION

Figure 2 displays the IRMPD spectra of the five HisGly complexes investigated here. The first goal is to assign the predominant overall binding motifs. Binding of metal ions to small gas-phase peptides has been considered in terms of three principal binding motifs, namely charge solvated (CS), zwitterion (ZW), and iminol (Im). The HisGly ligand combines with the present set of representative metal ions to give instances of complexes having CS and Im binding, but probably no ZW occurrences. Structures with binding to the $\tau$ nitrogen of the imidazole ring were not considered, as previous calculations had shown these to have much higher energies than binding to the $\pi$ nitrogen.[26] Previous studies of

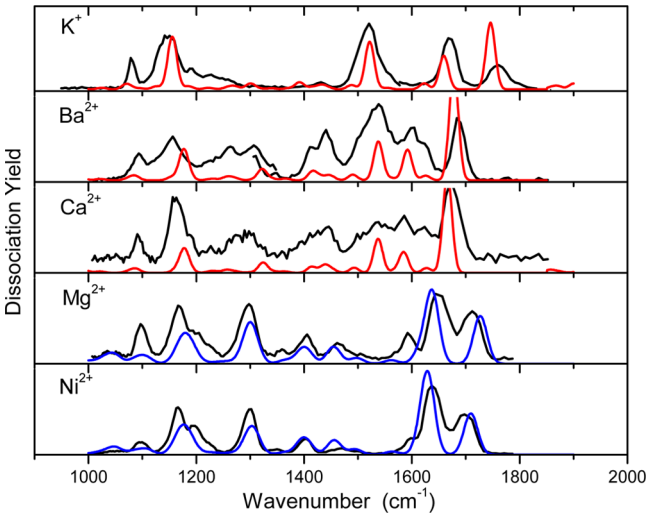


**Figure 2.** IRMPD spectra of the five HisGly complexes (black). The computed lowest energy structures are CS for the K, Ba, and Ca complexes, shown as red traces, and iminol for the Mg and Ni complexes, shown as blue traces.

dipeptides[26,27,34,36,37,42,43,47,58−63] give useful perspectives on the most likely structural patterns and their characteristic spectroscopic features, but the most reliable approach is by comparison of the observed spectra with computed IR spectra, as has been done in many previous IRMPD spectroscopy studies.[38−40,46]

It was found in previous studies of metal ion/peptide complexes[27,63] that the CS binding configuration is clearly signaled by a prominent IR feature in the 1500−1550 $cm^{-1}$ region corresponding mainly to the N−H bend of the proton on the amide nitrogen (the well-known amide II band). The clear identity of this diagnostic peak gives a good starting point for the interpretation of the present series of spectra. The spectra indicate the same progression from CS to iminol structures with increasing binding strength of the metal ion partner (Table 1) as was found for the PhePhe series.[27] The CS conformation is dominant for the $K^+$, $Ba^{2+}$, and $Ca^{2+}$ complexes, and absent for the $Mg^{2+}$ and $Ni^{2+}$ complexes. The correctness of the CS assignment for the former, as well as the assurance that the latter two complexes do in fact possess an iminol

**Table 1. Binding Affinities $\Delta H_0$ and $\Delta G_{298}$ (kJ/mol) and Bonding Distances (Å) of the Metal Ions toward HisGly[a]**

| | binding[b] | $\Delta H_0$ | $\Delta G_{298}$ | $R_{M-O}$ | $R_{M-N}$ |
|---|---|---|---|---|---|
| $K^+$ | CS | −196.4 | −163.2 | 2.673 | 2.789 |
| $Na^+$ | CS | −273.4 | −238.1 | 2.297 | 2.371 |
| $Li^+$ | CS (8) | −374.9 | −338.6 | 1.937 | 2.001 |
| $Ba^{2+}$ | CS (39) | −582.5 | −543.6 | 2.627 | 2.746 |
| $Ca^{2+}$ | CS (15) | −786.5 | −745.8 | 2.278 | 2.382 |
| $Mg^{2+}$ | Im (−15) | −1087.2 | −1045.7 | 2.048 | 2.064 |
| $Ni^{2+}$ | Im (−42) | −1359.2 | −1314.4 | 2.039 | 1.976 |
| $Ga^{3+}$ | Im (−22) | −2933 | −2886 | 1.913 | 1.894 |

[a] $R_{M-O}$ is the metal−carboxyl carbonyl oxygen distance, and $R_{M-N}$ is the metal−imidazole nitrogen distance. [b] Mode of binding of lowest energy isomer. Values in parentheses show the extent of binding preference, giving the energy of the lowest iminol minus the energy of the lowest CS isomer. The $Na^+$ and $K^+$ ions have no low-energy iminol forms.


dx.doi.org/10.1021/jp4021917 | J. Phys. Chem. A 2013, 117, 5335−5343

structure, will be further confirmed by the detailed matching with computational results described in the following.

Figures S1−S7 in the Supporting Information display the low-energy isomers and their spectra as found computationally, correlated with the experimental results. More briefly, Figure 2 shows the computed spectrum of the lowest energy isomer in each case. The agreement of experiment with the spectrum computed for the lowest energy structure is good in all five complexes, strongly suggesting that the predicted structure constitutes at least the major fraction of the ions in the trapped ion population.

The potassium ion complex displays the typical form of a CS di- or tripeptide complex,[34,42] with the trio of strong features in the high frequency region due to COOH carbonyl (1780 $cm^{-1}$), amide CO (1660 $cm^{-1}$), and amide NH (1530 $cm^{-1}$) vibrations, along with the strong peak (1150 $cm^{-1}$) due to C-terminal OH bending. The COOH carbonyl stretch (1780 $cm^{-1}$) is not quite correctly predicted, but the difference of 15 $cm^{-1}$ between experiment and prediction is well within the range of experience for the uncertainty of such predictions.

The moderately strong peak at 1080 $cm^{-1}$, which appears in all spectra, is at least partly due to the pyrrolic CH in-plane bend, and is the only major peak in this series of spectra that directly manifests the presence of the imidazole side chain. The intensity of this vibration is apparently not well treated by the calculations, which predict rather weak IR absorptions at this wavelength, although the frequency is well reproduced. For reference, this is the region of the strongest peak in the imidazole IR spectrum.[64]

The complexes with the alkaline earths $Ba^{2+}$ and $Ca^{2+}$ give spectra that are similar to each other, suggesting similar ion populations. As Figure 2 shows, the CS structure [CS $OON_i$] accounts for most of the features in the spectra. The CS $OONN_i$ structure for the calcium spectrum will be seen in the following to be slightly above the lowest energy CS $OON_i$ structure energetically, and is spectroscopically very similar to it, so a mixture of these two is quite likely, which would account for the rather cluttered appearance of this spectrum.

The spectra of the $Mg^{2+}$ and $Ni^{2+}$ complexes are again quite similar to each other, suggesting similar structures. In these cases, agreement with the predictions for the lowest energy iminol structure [Im $ONNN_i$] is highly satisfactory, and we confidently assign an iminol structure to both complexes.

With these assignments we can sum up the nature of the corresponding vibrational modes as shown in Figure 3. Here the spectra are labeled with the normal mode assignments based on the lowest energy calculated spectrum.

**Comparison with Other Dipeptides: PhePhe Complexes.** Data collected at FELIX now encompass series of metal ion complex spectra for three different dipeptide ligand types, HisGly as presented herein, PheAla[42,58,63] (along with PheGly), and PhePhe,[27,37] presenting differing active side-chain/metal interaction situations. All of these include a side chain at the N-terminus that is favorably situated to chelate the metal ion. The His side chain is a strongly complexing N-donor (lone pair of electrons on an imidazole nitrogen) with rather tight geometrical constraints around the metal ion in the effective region of lone-pair interaction, while the side chain of Phe offers a somewhat weaker interaction, where the donor $\pi$ cloud above the phenyl ring allows considerable positional flexibility for metal ion complexation on the flat $\pi$ surface. The role of cation−$\pi$ interactions with the ring of an aromatic amino acid residue (as with the Phe residue of interest here)

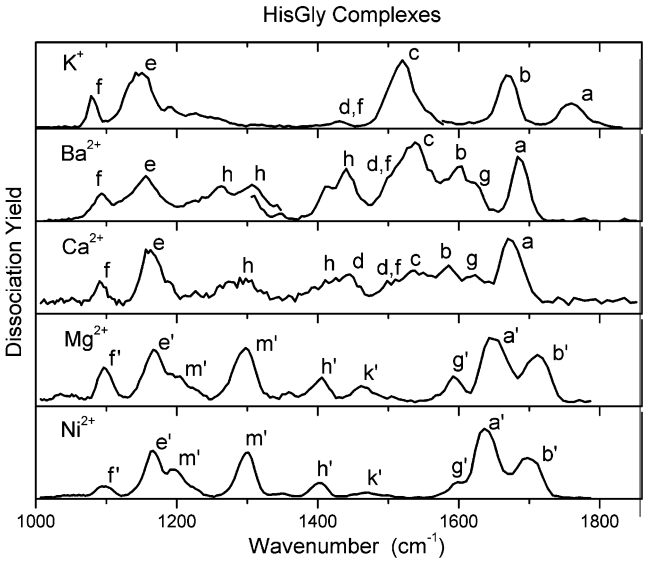


**Charge Solvated**
- a COOH carbonyl stretch
- b Amide carbonyl stretch
- c Amide NH bend
- d Pyrrole NH bend
- e COOH OH bend
- f Pyrrole CH bend
- g $NH_2$ scissors
- h $CH_2$ bends

**Iminol**
- a′ COOH carbonyl stretch
- b′ amide CN stretch
- e′ COOH OH bend
- f′ pyrrole CH; $NH_2$ scissors
- g′ $NH_2$ scissors
- h′ $CH_2$ bends
- k′ COOH COH stretch/bend
- m′ bends, CH and amide OH

**Figure 3.** Spectra of the five $M^{n+}$HisGly complexes, keyed to the computed normal mode positions of predicted strong peaks of low-energy conformations of different types. The computed spectra themselves are displayed in the Supporting Information.

has been extensively discussed as important to the structures and energetics of metal ion complexed peptides (see refs 13, 34, and 65−67 for a sample). The C-terminal aromatic side chain of PhePhe can give a second cation−$\pi$ interaction, making the comparison of the single-side-chain ligands versus this ligand slightly imperfect; however, this second ring chelation site in PhePhe has been found in calculations to interact more weakly with the metal ions compared with the N-terminal side chain, giving the present comparisons reasonable validity.

It is most useful to start with the comparison of HisGly with PhePhe, since the well-constrained geometries of PhePhe complexes give cleaner, more easily interpreted spectra than the more flexible PheAla (PheGly) complexes. The five PhePhe spectra have been published and are well understood.[27,37] In Figure 4 the corresponding PhePhe and HisGly spectra are overlaid.

The spectra for the HisGly and PhePhe complexes with potassium (Figure 4, top panel) show substantial similarity, and both spectra are attributed to a CS structure. The spectra of complexes with the alkaline earth ions $Ba^{2+}$ and $Ca^{2+}$ also show substantial similarity between HisGly and PhePhe. Both PhePhe complexes were confidently assigned as CS OORR structures.[37] The HisGly complexes give more congested spectra and show more peak broadening, and it seems that these complexes do not have the structural rigidity that leads to the remarkably fine PhePhe spectra; nevertheless, the spectra are similar in most of their overall features, and probably reflect similar CS structures (CS OORR and CS $OON_i$, for PhePhe and HisGly respectively) for the major fraction of the


dx.doi.org/10.1021/jp4021917 | J. Phys. Chem. A 2013, 117, 5335−5343

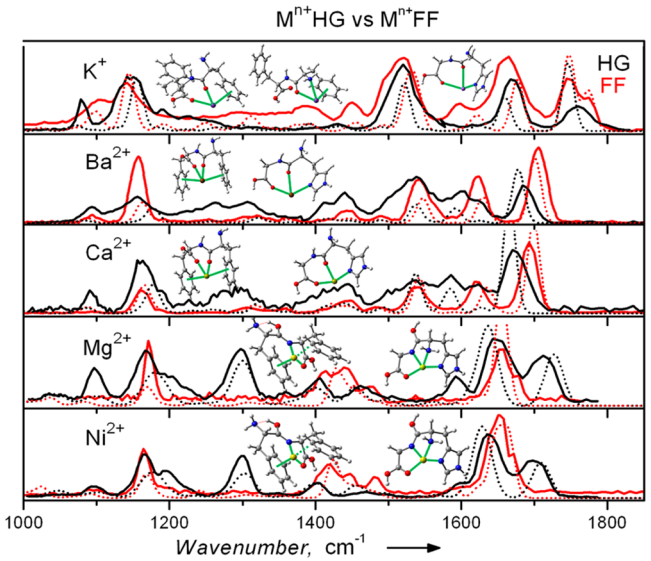


**Figure 4.** Comparison of complexes of HisGly with those of PhePhe. Black traces are HisGly; red traces are PhePhe. The solid lines are the experimental spectra, and the dotted lines are the computed spectra of the conformers assigned as likely structures corresponding to the observed ions, which are shown in the structure diagrams in each panel. (See refs 27 and 37 for assignments of PhePhe complexes. The $K^+$PhePhe complex was modeled in ref 37 as a nearly equal mixture of the two CS structures shown. The red dotted trace is a composite of these two spectra.)

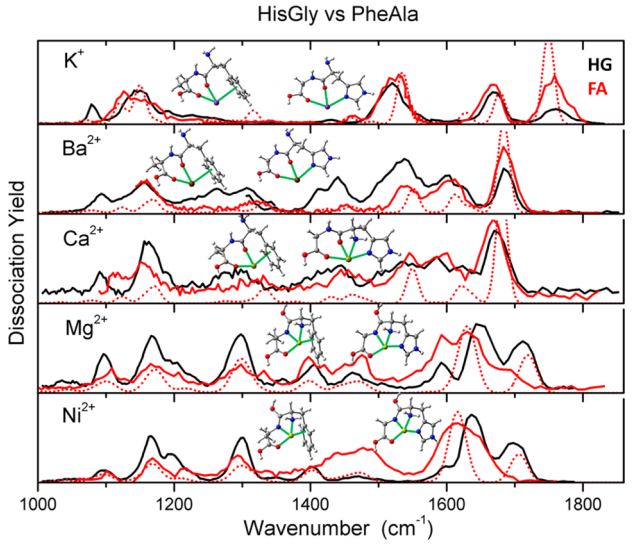


**Figure 5.** Comparison of HisGly and PheAla metal ion complexes. Black traces are experimental data for HisGly complexes, red solid traces are experimental data for PheAla complexes, and dotted red traces are computed spectra for what is surmised to be the most abundant conformation of the corresponding PheAla complex.

populations. The most obvious differences are the two carbonyl-based vibrational modes (1670 and 1580 $cm^{-1}$ in $Ca^{2+}$HisGly) which are noticeably red-shifted in the HisGly complexes compared with the PhePhe complexes. These shifts are well reproduced by the DFT results.

Most interesting is the strong contrast between the HisGly and the PhePhe complexes of the strong-binding metal ions $Mg^{2+}$ and $Ni^{2+}$. All four of these complexes are clearly iminol complexes, as signaled by the absence of the amide II peak (1500−1550 $cm^{-1}$). However, the PhePhe complexes are distinguished by the absence of two strong features near 1700 and 1300 $cm^{-1}$ that are prominent in the HisGly spectra. As is confirmed by the excellent agreement of all of these spectra with the respective computations, the difference between these ligands lies in the fact that the terminal amino group chelates the metal ion in the HisGly cases (Im $ONNN_i$), while this group lies distant from the metal and forms a strong hydrogen bond to the iminol OH proton in the PhePhe complexes (Im ONRR, Figure 4). This difference is readily understood in terms of excessive steric crowding around the metal in the PhePhe cases in attempts to form an Im ONNRR pentacoordinate chelate. The 1700 $cm^{-1}$ peak visible in the HisGly complexes is the iminol C−N stretch (which also involves OH bending of the iminol proton); this peak is red-shifted by about 50 $cm^{-1}$ in the PhePhe systems so that it overlaps with the amide CO stretch near 1650 $cm^{-1}$ and is not seen as a distinct peak. The 1300 $cm^{-1}$ normal mode in the HisGly complexes has in part the character of the OH bending motion of the (free) iminol proton; this motion is strongly perturbed in the H-bonded PhePhe complexes, causing a suppression of the 1300 $cm^{-1}$ peak in their spectra.

**Comparison with Other Dipeptides: PheAla (PheGly) Complexes.** Comparison of the spectra of complexes of HisGly with those of PheAla (Figure 5) is parallel in many respects to the comparison with PhePhe. The $K^+$PheAla spectrum has been published and discussed previously.[42] The other PheAla complex spectra have been published most recently,[62] but without calculations or detailed discussion, so they are reproduced in Figures S8−S11 in the Supporting Information. Spectral comparisons are summarized in Figure 5. The PheAla complexes of the three weaker-binding metal ions ($K^+$, $Ba^{2+}$, and $Ca^{2+}$) gave spectra similar to the HisGly spectra, and are interpreted as CS complexes having the CS OOR structure. The $Ca^{2+}$PheAla spectrum was congested and poorly resolved similar to the $Ca^{2+}$HisGly case, in striking contrast to the excellent, well-resolved $Ca^{2+}$PhePhe spectrum. For both PheAla and HisGly ligands, $Ca^{2+}$ is apparently a metal ion without a single strongly preferred ground state structure of the complexes, with the spectra reflecting mixtures of structures and thereby making interpretation difficult. As was noted for PheAla in ref 63, the substantial intensity of the amide NH bending vibration around 1530 $cm^{-1}$ in both $Ca^{2+}$ spectra indicates at least a large contribution from the CS structure. Unlike for $Ca^{2+}$AlaAla (ref 63), the poor match of ZW calculated spectra with the $Ca^{2+}$PheAla experimental spectrum and the high energy of the ZW structures (see Figure S9 in the Supporting Information) suggests little or no ZW contribution for $Ca^{2+}$PheAla, and the same is true for $Ca^{2+}$HisGly. An iminol contribution to the $Ca^{2+}$PheAla spectrum is energetically and spectroscopically unfavorable (Figure S9 in the Supporting Information), but for $Ca^{2+}$HisGly, the Im $ONNN_i$ iminol structure is a bit less unfavorable, and may make a contribution: this latter structure lies only 14.5 kJ $mol^{-1}$ above the ground state CS structure and offers a good explanation for the observed intensity around 1250−1300 $cm^{-1}$ (see Figure S3 in the Supporting Information).

The PheAla spectra of $Mg^{2+}$ and $Ni^{2+}$ are similar to each other, but they differ quite markedly from the corresponding HisGly spectra in the 1600−1750 $cm^{-1}$ region. We will make tentative structure assignments for the PheAla cases for magnesium and nickel, but leave open other possibilities. As indicated above, the HisGly ligand for both of these metal ions


dx.doi.org/10.1021/jp4021917 | J. Phys. Chem. A 2013, 117, 5335−5343

gives spectra fully consistent with the calculated Im ONNN$_i$ conformation, which is predicted to be the lowest energy structure, giving confidence in the HisGly assignments of $Mg^{2+}$HisGly and $Ni^{2+}$HisGly complexes as Im ONNN$_i$. The PheAla spectra are in excellent agreement with those calculated for the lowest energy structures of Im ONNR, except in the high-frequency region between 1550 and 1750 cm$^{-1}$ (see Figures S10 and S11 in the Supporting Information). In particular, the expected iminol C−N stretching mode, predicted above 1700 cm$^{-1}$, appears to be strongly red-shifted and weakened compared with the calculations. Alternatively, it is possible to assign the predominant conformations of the PheAla complexes to the Im ONR_OH hydrogen-bonded structures displayed in Figures S10 and S11 in the Supporting Information (analogous to the corresponding PhePhe complexes). The Im ONR_OH structures, especially in the nickel case, can account for the strongly red-shifted iminol C−N stretch, although otherwise they do not match the experimental spectra as well as Im ONNR, so they cannot be entirely ruled out. To summarize the situation with respect to the structures of the PheAla complexes of $Mg^{2+}$ and $Ni^{2+}$, their spectra do not agree very well with the corresponding HisGly complexes or with calculations. Unlike the HisGly versus PhePhe comparisons noted above, we cannot reach unambiguous conformational conclusions. The assignment of the PheAla complex structures remains uncertain pending further clarification, perhaps by spectroscopy in the hydrogen-stretching region above 3000 cm$^{-1}$.

**Additional Calculations for $Li^+$ and $Ga^{3+}$ Complexes.** HisGly complexes of two metal ions with small bonding radii (Table 1) comparable to $Ni^{2+}$ and $Mg^{2+}$ but with different charges, namely $Li^+$ and $Ga^{3+}$, were computationally investigated although their experimental spectra were not recorded. These results are shown in the Supporting Information. $Li^+$, the strongest-binding alkali metal ion, might be the most likely singly charged metal ion to form an iminol structure. However, the calculated $Li^+$ complex with the lowest energy has an entirely normal tridentate CS OON$_i$ structure analogous to the $K^+$ complex (Figures S6 and S14 in the Supporting Information). The alternative tridentate structures CS ONN$_i$ are higher by 17.4 and 38.8 kJ mol$^{-1}$, and the lowest iminol structure is higher by 40.8 kJ mol$^{-1}$. Analogous to the stronger-binding +2 metal ions, it might be expected that the tetradentate CS OONN$_i$ structure would also be relatively more favorable among CS structures for $Li^+$. However, in fact the calculations show that this latter structure is less favorable than the tridentate structures, indicating that the high ligand binding energy of the $Li^+$ ion is outweighed by the unfavorability of crowding four ligands around this small ion center.

Low-energy calculated structures of $Ga^{3+}$HisGly are shown in Figures S7 and S19 in the Supporting Information. Experimental knowledge about triply charged peptide complexes is sparse, although there have been numerous studies of doubly charged deprotonated ions derived from triply charged species (for example, the complexes of trivalent lanthanide ions with deprotonated peptides reported by Prell et al.[44]). Some preliminary structures of $La^{3+}$ complexes of arginine-containing peptides have also been proposed although iminol-type structures were not recognized as important.[68] Recently the first detailed structural studies of triply charged La complexes with an amino acid were reported, utilizing both DFT calculations and IRMPD spectroscopy of lanthanum ions coordinated to derivatized tryptophan.[69] However, triply charged complexes analogous to the singly and doubly charged complexes of ligands containing an amide linkage considered in the present work have yet to be characterized. The present calculation of the gallium complex thus represents an interesting predicted structure of this yet-to-be observed species. The computation of the $Ga^{3+}$ complex shown in Figure S19 in the Supporting Information indicates a definite preference for the tetradentate iminol structure Im ONNN$_i$, similar to the preferred iminol structures of the $Mg^{2+}$ and $Ni^{2+}$ complexes (Figures S4 and S5 in the Supporting Information). Thus it seems likely that the iminol tautomerization leading to the dominant iminol structure for the $Mg^{2+}$ and $Ni^{2+}$ complexes will also be dominant in comparable triply charged complexes.

## ■ CONCLUSIONS

The nickel and magnesium HisGly complexes illustrate two points of difference between solution and gas phase. First, the gas phase gives a greater preference for deprotonation of the amide nitrogen and formation of a metal−nitrogen bond. In solution the choice between CS binding and amide nitrogen deprotonation appears to be close, depending on which metal is involved, but in the gas phase, the iminol binding mode is strongly preferred for both nickel and magnesium ions. Second, the gas-phase complex, with no available chelating agent other than the single ligand, allows simultaneous chelation by all four available Lewis basic sites, including three nitrogen atoms. By contrast, in solution even metal ions such as Cu(II) which can deprotonate the amide nitrogen (which Ni(II) does not do) still do not bind all three nitrogen sites, instead completing the metal ion coordination by bringing in a second ligand or by binding water molecules.[11,31,33]

Reflecting the similarity of complexation for dipeptides having imidazole versus phenyl chelation sides at the N-terminus, the preferred conformations are often parallel among the three ligand types compared here. For $K^+$ the parallel tridentate conformations CS OON$_i$ and CS OOR are favored. For $Ba^{2+}$ the tetradentate conformations (CS OONN$_i$ and CS OONR) are almost indistinguishable on spectroscopic and thermochemical grounds from the respective tridentate conformations (CS OON$_i$ and CS OOR) for HisGly and PheAla, but the tetradentate encapsulated conformation CS OORR is clearly best for PhePhe. Similarly, $Ca^{2+}$ is firmly encapsulated in the CS OORR conformation for PhePhe, but for this metal ion with HisGly and PheAla the tetradentate structures CS OON$_a$N$_i$ and CS OON$_a$R are not clearly distinguishable from the respective tridentate CS OON$_i$ and CS OOR conformations. For $Ca^{2+}$HisGly and $Ca^{2+}$PhePhe, there is also a possibility of a fractional presence of iminol conformation (Im ONNN or Im ON$_a$RR), while for $Ca^{2+}$PheAla a significant iminol contribution is not in evidence.

Considering the nickel and magnesium ion complexes, we note that the corresponding complexes of these two metals are spectroscopically very similar to each other. With HisGly and PhePhe, both metal ions give unequivocal tetradentate iminol structures although an important distinction is that with HisGly (Im ONNN) the fourth binding site is the amino nitrogen, while with PhePhe (Im ONRR) the amino nitrogen is free (forming a remote hydrogen bond) and replaced by the C-terminal phenyl ring. With PheAla, we also assign tetradentate iminol structures (Im ONNR), but cannot rule out the possible alternative of tridentate iminol (Im ONR).


dx.doi.org/10.1021/jp4021917 | J. Phys. Chem. A 2013, 117, 5335−5343

As a general conclusion, CS structures are preferred for the weak-binding metal ions $K^+$, $Ba^{2+}$, and $Ca^{2+}$, while iminol structures are preferred for the strong-binding metals $Mg^{2+}$ and $Ni^{2+}$. It is notable that, with all three ligand types considered here, the metal ion complexes group into three well-defined spectroscopic patterns. The nickel and magnesium complexes give nearly indistinguishable spectra. Similarly, the calcium and barium complexes are often nearly indistinguishable (but quite distinct from the nickel/magnesium pattern.) The potassium complexes are again distinct from all the divalent metal ion complexes. The governing principles dividing these spectroscopic groups have been discussed herein in terms of (1) the differing propensities for choosing the iminol binding pattern, and (2) the major spectroscopic significance of single versus double charge on the metal center. Particularly noteworthy is the observation of similar gas-phase binding behaviors of nickel and magnesium ions, contrasting with their quite different patterns of peptide interaction in condensed phases.

## ■ ASSOCIATED CONTENT

### Supporting Information

Computed spectra of HisGly and PheAla complexes; structure diagrams of HisGly complexes. This material is available free of charge via the Internet at http://pubs.acs.org.

## ■ AUTHOR INFORMATION

### Corresponding Author

*E-mail: rcd@po.cwru.edu (R.C.D.); joso@science.ru.nl (J.O.); kwmsiu@yorku.ca (K.W.M.S.). Tel.: (216) 368-3712 (R.C.D.). Fax: (216) 368-3006 (R.C.D.).

### Notes

The authors declare no competing financial interest.

## ■ ACKNOWLEDGMENTS

This work was financially supported by the "Nederlandse Organisatie voor Wetenschappelijk Onderzoek" (NWO). R.C.D. acknowledges support from the National Science Foundation, Grant PIRE-0730072, and expresses gratitude to the FELIX facility for its continuing welcome. The FELIX staff, and particularly Dr. Lex van der Meer and Dr. Britta Redlich, are gratefully acknowledged for their assistance. We thank SURFsara Computing and Networking Services (www.surfsara.nl) for their support in using the Lisa Compute Cluster. A.C.H. and K.W.M.S. acknowledge support by the Natural Sciences and Engineering Reseach Council of Canada. This study was made possible by the FELIX infrastructure and the facilities of the Shared Hierarchical Academic Research Computing Network (http://www.sharcnet.ca) and the High Performance Computing Virtual Laboratory (http://www.hpcvl.org).

## ■ REFERENCES

(1) Loo, J. A.; Hu, P. F.; Smith, R. D. Interaction of Angiotensin Peptides and Zinc Metal-Ions Probed by Electrospray-Ionization Mass Spectrometry. *J. Am. Soc. Mass Spectrom.* **1994**, *5*, 959−965.

(2) Sarkar, B.; Wigfield, Y. The structure of copper(II)histidine chelate. *J. Biol. Chem.* **1967**, *242*, 5572−5577.

(3) Sovago, I.; Osz, K. Metal Ion Selectivity of Oligopeptides. *Dalton Trans.* **2006**, 3841−3854.

(4) Timari, S.; Kallay, C.; Osz, K.; Sovago, I.; Varnagy, K. Transition Metal Complexes of Short Multihistidine Peptides. *Dalton Trans.* **2009**, 1962−1971.

(5) Lewis, E. A.; Tolman, W. B. Reactivity of Dioxygen-Copper Systems. *Chem. Rev.* **2004**, *104*, 1047−1076.

(6) Ali-Torres, J.; Marechal, J. D.; Rodriguez-Santiago, L.; Sodupe, M. Three Dimensional Models of $Cu^{2+}$-A$\beta$(1-16) Complexes from Computational Approaches. *J. Am. Chem. Soc.* **2011**, *133*, 15008−15014.

(7) Sundberg, R. J.; Martin, R. B. Interactions of Histidine and Other Imidazole Derivatives with Transition-Metal Ions in Chemical and Biological Systems. *Chem. Rev.* **1974**, *74*, 471−517.

(8) Martin, R. B. Bioinorganic Chemistry of Calcium. In *Metal Ions in Biological Systems: Probing of Proteins by Metal Ions and Their Low-Molecular-Weight Complexes*; Sigel, A., Sigel, H., Eds.; Marcel Dekker: New York, 1984; Vol. *17*, pp 1−49.

(9) Martin, R. B. Peptide Bond Characteristics. In *Metal Ions in Biological Systems: Probing of Proteins by Metal Ions and their Low-Molecular-Weight Complexes*; Sigel, A., Sigel, H., Eds.; Marcel Dekker: New York, 2001; Vol. *38*, pp 1−23.

(10) Martin, R. B.; Chamberlin, M.; Edsall, J. T. The Association of Nickel(II) Ion with Peptides. *J. Am. Chem. Soc.* **1960**, *82*, 495−498.

(11) Sigel, H.; Martin, R. B. Coordinating Properties of the Amide Bond. Stability and Structure of Metal Ion Complexes of Peptides and Related Ligands. *Chem. Rev.* **1982**, *82*, 385−426.

(12) Margerum, D. W., Dukes, G. R. Kinetics and Mechanisms of Metal-Ion and Proton-Transfer Reactions of Oligopeptide Complexes. In *Metal Ions in Biological Systems: Simple Complexes*; Sigel, A., Sigel, H., Eds.; Marcel Dekker: New York, 1974; Vol. *1*; p 158.

(13) Ma, J. C.; Dougherty, D. A. The Cation-$\pi$ Interaction. *Chem. Rev.* **1997**, *97*, 1303−1324.

(14) Dunbar, R. C.; Hopkinson, A. C.; Oomens, J.; Siu, C. K.; Siu, K. W. M.; Steill, J. D.; Verkerk, U. H.; Zhao, J. F. Conformation Switching in Gas-Phase Complexes of Histidine with Alkaline Earth Ions. *J. Phys. Chem. B* **2009**, *113*, 10403−10408.

(15) Citir, M.; Hinton, C. S.; Oomens, J.; Steill, J. D.; Armentrout, P. B. Infrared Multiple Photon Dissociation Spectroscopy of Cationized Histidine: Effects of Metal Cation Size on Gas-Phase Conformation. *J. Phys. Chem. A* **2012**, *116*, 1532−1541.

(16) Hofstetter, T. E.; Howder, C.; Berden, G.; Oomens, J.; Armentrout, P. B. Structural Elucidation of Biological and Toxicological Complexes: Investigation of Monomeric and Dimeric Complexes of Histidine with Multiply Charged Transition Metal (Zn and Cd) Cations Using IR Action Spectroscopy. *J. Phys. Chem. B* **2011**, *115*, 12648−12661.

(17) Citir, M.; Hinton, C. S.; Oomens, J.; Steill, J. D.; Armentrout, P. B. Infrared Multiple Photon Dissociation Spectroscopy of Protonated Histidine and 4-Phenyl Imidazole. *Int. J. Mass Spectrom.* **2012**, *330*, 6−15.

(18) O'Brien, J. T.; Prell, J. S.; Berden, G.; Oomens, J.; Williams, E. R. Effects of Anions on the Zwitterion Stability of Glu, His and Arg Investigated by IRMPD Spectroscopy and Theory. *Int. J. Mass Spectrom.* **2010**, *297*, 116−123.

(19) Steill, J.; Zhao, J. F.; Siu, C. K.; Ke, Y. Y.; Verkerk, U. H.; Oomens, J.; Dunbar, R. C.; Hopkinson, A. C.; Siu, K. W. M. Structure of the Observable Histidine Radical Cation in the Gas Phase: A Captodative alpha-Radical Ion. *Angew. Chem., Int. Ed.* **2008**, *47*, 9666−9668.

(20) Prell, J. S.; O'Brien, J. T.; Steill, J. D.; Oomens, J.; Williams, E. R. Structures of Protonated Dipeptides: The Role of Arginine in Stabilizing Salt Bridges. *J. Am. Chem. Soc.* **2009**, *131*, 11442−11449.

(21) Lucas, B.; Gregoire, G.; Lemaire, J.; Maître, P.; Glotin, F.; Schermann, J. P.; Desfrancois, C. Infrared Multiphoton Dissociation Spectroscopy of Protonated N-Acetyl-alanine and Alanyl-histidine. *Int. J. Mass Spectrom.* **2005**, *243*, 105−113.

(22) Armentrout, P. B.; Citir, M.; Chen, Y.; Rodgers, M. T. Thermochemistry of Alkali Metal Cation Interactions with Histidine: Influence of the Side Chain. *J. Phys. Chem. A* **2012**, *116*, 11823−11832.

(23) Chen, Y.; Rodgers, M. T. Structural and Energetic Effects in the Molecular Recognition of Acetylated Amino Acids by 18-Crown-6. *J. Am. Soc. Mass Spectrom.* **2012**, *23*, 2020−2030.

(24) Wang, P.; Ohanessian, G.; Wesdemiotis, C. The Sodium Ion Affinities of Asparagine, Glutamine, Histidine and Arginine. *Int. J. Mass Spectrom.* **2008**, *269*, 34−45.

(25) Lavanant, H.; Hecquet, E.; Hoppilliard, Y. Complexes of L-histidine with Fe2+, Co2+, Ni2+, Cu2+, Zn2+ Studied by Electrospray Ionization Mass Spectrometry. *Int. J. Mass Spectrom.* **1999**, *185*, 11−23.
(26) Kapota, C.; Ohanessian, G. The Low Energy Tautomers and Conformers of the Dipeptides HisGly and GlyHis and of Their Sodium Ion Complexes in the Gas Phase. *Phys. Chem. Chem. Phys.* **2005**, *7*, 3744−3755.
(27) Dunbar, R. C.; Steill, J. D.; Polfer, N. C.; Berden, G.; Oomens, J. Peptide Bond Tautomerization Induced by Divalent Metal Ions: Emergence of the Iminol Configuration. *Angew. Chem., Int. Ed.* **2012**, *51*, 4591−4593.
(28) Rodriquez, C. F.; Fournier, R.; Chu, I. K.; Hopkinson, A. C.; Siu, K. W. M. A Possible Origin of [M-nH+mX]((m-n)+) Ions (X = Alkali Metal Ions) in Electrospray Mass Spectrometry of Peptides. *Int. J. Mass Spectrom.* **1999**, *192*, 303−317.
(29) Rodriquez, C. F.; Guo, X.; Shoeib, T.; Hopkinson, A. C.; Siu, K. W. M. Formation of [M-nH+mNa]((m-n)+) and [M-nH+mK]((m-n)+) Ions in Electrospray Mass Spectrometry of Peptides and Proteins. *J. Am. Soc. Mass Spectrom.* **2000**, *11*, 967−975.
(30) Grewal, R. N.; Aribi, H. E.; Simth, J. C.; Rodriquez, C. F.; Hopkinson, A. C.; Siu, K. W. M. Multiple Substitution of Protons by Podium Ions in Sodiated Oligoglycines. *Int. J. Mass Spectrom.* **2002**, *219*, 89−99.
(31) Brookes, G.; Pettit, L. D. Thermodynamics of Formation of Complexes of Copper(II) and Nickel(II) with Glycylhistidine, Beta-Alanylhistidine, and Histidylglycine. *J. Chem. Soc., Dalton Trans.* **1975**, 2112−2117.
(32) Aiba, H.; Yokoyama, A.; Tanaka, H. Copper(II) Complexes of L-HistidylGlycine and L-HistidylGlycylGlycine in Aqueous Solutions. *Bull. Chem. Soc. Jpn.* **1974**, *47*, 136−142.
(33) Conato, C.; Ferrari, S.; Kozlowski, H.; Pulidori, F.; Remelli, M. Ni(II) Complexes of Dipeptides: A Thermodynamic and Spectroscopic Study. *Polyhedron* **2001**, *20*, 615−621.
(34) Dunbar, R. C.; Steill, J. D.; Oomens, J. Conformations and Vibrational Spectroscopy of Metal Ion/Polylalanine Complexes. *Int. J. Mass Spectrom.* **2010**, *297*, 107−115.
(35) Oomens, J.; Sartakov, B. G.; Meijer, G.; von Helden, G. Gas-Phase Infrared Multiple Photon Dissociation Spectroscopy of Mass-Selected Molecular Ions. *Int. J. Mass Spectrom.* **2006**, *254*, 1−19.
(36) Balaj, O. P.; Kapota, C.; Lemaire, J.; Ohanessian, G. Vibrational Signatures of Sodiated Oligopeptides (GG-Na+, GGG-Na+, AA-Na+ and AAA-Na+) in the Gas Phase. *Int. J. Mass Spectrom.* **2008**, *269*, 196−209.
(37) Dunbar, R. C.; Steill, J. D.; Oomens, J. Encapsulation of Metal Cations by the PhePhe Ligand: A Cation-$\pi$ Ion Cage. *J. Am. Chem. Soc.* **2011**, *133*, 9376−9386.
(38) Eyler, J. R. Infrared Multiple Photon Dissociation Spectroscopy of Ions in Penning Traps. *Mass Spectrom. Rev.* **2009**, *28*, 448−467.
(39) Fridgen, T. D. Infrared Consequence Spectroscopy of Gaseous Protonated and Metal Ion Cationized Complexes. *Mass Spectrom. Rev.* **2009**, *28*, 586−607.
(40) Polfer, N. C.; Oomens, J. Vibrational Spectroscopy of Bare and Solvated Ionic Complexes of Biological Relevance. *Mass Spectrom. Rev.* **2009**, *28*, 468−494.
(41) Oomens, J.; Polfer, N.; Moore, D. T.; van der Meer, L.; Marshall, A. G.; Eyler, J. R.; Meijer, G.; von Helden, G. Charge-State Resolved Mid Infrared Spectroscopy of a Gas-Phase Protein. *Phys. Chem. Chem. Phys.* **2005**, *7*, 1345−1348.
(42) Polfer, N. C.; Oomens, J.; Dunbar, R. C. Alkali Metal Complexes of the Dipeptides PheAla and AlaPhe: IRMPD Spectroscopy. *ChemPhysChem* **2008**, *9*, 579−589.
(43) Prell, J. S.; Demireva, M.; Oomens, J.; Williams, E. R. Role of Sequence in Salt-Bridge Formation for Alkali Metal Cationized GlyArg and ArgGly Investigated with IRMPD Spectroscopy and Theory. *J. Am. Chem. Soc.* **2009**, *131*, 1232−1242.
(44) Prell, J. S.; Flick, T. G.; Oomens, J.; Berden, G.; Williams, E. R. Coordination of Trivalent Metal Cations to Peptides: Results from IRMPD Spectroscopy and Theory. *J. Phys. Chem. A* **2010**, *114*, 854−860.
(45) Semrouni, D.; Balaj, O. P.; Calvo, F.; Correia, C. F.; Clavaguéra, C.; Ohanessian, G. Structure of Sodiated Octa-Glycine: IRMPD Spectroscopy and Molecular Modeling. *J. Am. Soc. Mass Spectrom.* **2010**, *21*, 728−738.
(46) MacAleese, L.; Maitre, P. Infrared Spectroscopy of Organometallic Ions in the Gas Phase: From Model to Real World Complexes. *Mass Spectrom. Rev.* **2007**, *26*, 583−605.
(47) Dunbar, R. C.; Steill, J. D.; Oomens, J. Chirality-Induced Conformational Preferences in Peptide-Metal Ion Binding Revealed by IR Spectroscopy. *J. Am. Chem. Soc.* **2011**, *133*, 1212−1215.
(48) Rizzo, T. R.; Stearns, J. A.; Boyarkin, O. V. Spectroscopic Studies of Cold, Gas-Phase Biomolecular Ions. *Int. Rev. Phys. Chem.* **2009**, *28*, 481−515.
(49) Frisch, M. J.; Trucks, G. W.; Schlegel, H. B.; Scuseria, G. E.; Robb, M. A.; Cheeseman, J. R.; Montgomery, J. A., Jr.; Vreven, T.; Kudin, K. N.; Burant, J. C.; Millam, J. M.; Iyengar, S. S.; Tomasi, J.; Barone, V.; Mennucci, B.; Cossi, M.; Scalmani, G.; Rega, R.; Petersson, G. A.; Nakatsuji, H.; Hada, M.; Ehara, M.; Toyota, K.; Fukuda, R.; Hasegawa, J.; Ishida, M.; Nakajima, T.; Honda, Y.; Kitao, O.; Nakai, H.; Klene, M.; Li, X.; Knox, J. E.; Hratchian, H. P.; Cross, J. P.; Bakken, V.; Adamo, C.; Jaramillo, J.; Gomperts, R.; Stratmann, R. E.; Yazyev, O.; Austin, A. J.; Cammi, R.; Pomelli, C.; Ochterski, J. W.; Ayala, P. Y.; Morokuma, K.; Voth, G. A. Salvador, P.; Dannenberg, J. J.; Zakrzewski, V. G.; Dapprich, S.; Daniels, A. D.; Strain, M. C.; Farkas, O.; Malick, D. K.; Rabuck, A. D.; Raghavachari, K.; Foresman, J. B.; Ortiz, J. V.; Cui, Q.; Baboul, A. G.; Clifford, S.; Cioslowski, J.; Stefanov, B. B.; Liu, G.; Liashenko, A.; Piskorz, P.; Komaromi, I.; Martin, R. L.; Fox, D. J.; Keith, T.; Al-Laham, M. A.; Peng, C. Y.; Nanayakkara, A.; Challacombe, M.; Gill, P. M. W.; Johnson, B.; Chen, W.; Wong, M. W.; Gonzalez, C.; Pople, J. A. *Gaussian03*; Gaussian, Inc.: Wallingford, CT, 2004.
(50) Becke, A. D. Density-Functional Exchange-Energy Approximation with Correct Asymptotic Behavior. *Phys. Rev. B: Condens. Matter* **1988**, *A38*, 3098−3010.
(51) Becke, A. D. Density-Functional Thermochemistry 3. The Role of Exact Exchange. *J. Chem. Phys.* **1993**, *98*, 5648−5652.
(52) Becke, A. D. A New Mixing of Hartree-Fock and Local Density-Functional Theories. *J. Chem. Phys.* **1993**, *98*, 1372−1377.
(53) Chandrasekhar, J.; Andrade, J. G.; Schleyer, P. v. R. Efficient and Accurate Calculation of Anion Proton Affinities. *J. Am. Chem. Soc.* **1981**, *103*, 5609−5612.
(54) Hariharan, P. C.; Pople, J. A. Effect of D-Functions on Molecular-Orbital Energies for Hydrocarbons. *Chem. Phys. Lett.* **1972**, *16*, 217−219.
(55) Hehre, W. J.; Ditchfield, R.; Pople, J. A. Self-Consistent Molecular-Orbital Methods. 12. Further Extensions of Gaussian-Type Basis Sets for Use in Molecular-Orbital Studies of Organic Molecules. *J. Chem. Phys.* **1972**, *56*, 2257−2261.
(56) Lee, C. T.; Yang, W. T.; Parr, R. G. Development of the Colle-Salvetti Correlation-Energy Formula into a Functional of the Electron-Density. *Phys. Rev. B: Condens. Matter* **1988**, *37*, 785−789.
(57) Kaupp, M.; Schleyer, P. v. R.; Stoll, H.; Preuss, H. Pseudopotential Approaches to Ca, Sr and Ba Hydrides—Why Are Some Alkaline-Earth MX2 Compounds Bent? *J. Chem. Phys.* **1991**, *94*, 1360−1366.
(58) Dunbar, R. C.; Steill, J.; Polfer, N. C.; Oomens, J. Peptide Length, Steric Effects and Ion Solvation Govern Zwitterion Stabilization in Barium-Chelated Di- and Tripeptides. *J. Phys. Chem. B* **2009**, *113*, 10552−10554.
(59) Cerda, B. A.; Hoyau, S.; Ohanessian, G.; Wesdemiotis, C. $Na^+$ Binding to Cyclic and Linear Dipeptides. Bond Energies, Entropies of $Na^+$ Complexation, and Attachment Sites from the Dissociation of $Na^+$-Bound Heterodimers and ab Initio Calculations. *J. Am. Chem. Soc.* **1998**, *120*, 2437−2448.
(60) Wyttenbach, T.; Bushnell, J. E.; Bowers, M. T. Salt Bridge Structures in the Absence of Solvent? The Case for the Oligoglycines. *J. Am. Chem. Soc.* **1998**, *120*, 5098−5103.

(61) Benzakour, M.; McHarfi, M.; Cartier, A.; Daoudi, A. Interactions of Peptides with Metallic Cations. I. Complexes Glycylglycine-M+ (M=Li, Na). *J. Mol. Struct.: THEOCHEM* **2004**, *710*, 169−174.
(62) Kish, M.; Wesdemiotis, C.; Ohanessian, G. The Sodium Ion Affinity of Glycylglycine. *J. Phys. Chem. B* **2004**, *108*, 3086−3091.
(63) Dunbar, R. C.; Polfer, N. C.; Berden, B.; Oomens, J. Metal Ion Binding to Peptides: Oxygen or Nitrogen Sites? *Int. J. Mass Spectrom.* **2012**, *330*, 71−77.
(64) Coblentz Society, Inc. Evaluated Infrared Reference Spectra. In *NIST Chemistry WebBook*, NIST Standard Reference Database No. 69; Linstrom, P. J., Mallard, W. G., Eds.; National Institute of Standards and Technology: Gaithersburg, MD. http://webbook.nist.gov.
(65) Remko, M.; Fitz, D.; Broer, R.; Rode, B. M. Effect of Metal Ions ($Ni^{2+}$, $Cu^{2+}$ and $Zn^{2+}$) and Water Coordination on the Structure of L-Phenylalanine, L-Tyrosine, L-Tryptophan and Their Zwitterionic Forms. *J. Mol. Model.* **2011**, *17*, 3117−3128.
(66) Wu, R.; McMahon, T. B. Investigation of Cation-$\pi$ Interactions in Biological Systems. *J. Am. Chem. Soc.* **2008**, *130*, 12554−12555.
(67) Rimola, A.; Rodriguez-Santiago, L.; Sodupe, M. Cation-$\pi$ Interactions and Oxidative Effects on $Cu^{+}$ and $Cu^{2+}$ Binding to Phe, Tyr, Trp, and Its Amino Acids in the Gas Phase. Insights from First-Principles Calculations. *J. Phys. Chem. B* **2006**, *110*, 24189−24199.
(68) Shi, T.; Siu, K. W. M.; Hopkinson, A. C. Generation of $[La(peptide)]^{3+}$ Complexes in the Gas Phase: Determination of the Number of Binding Sites Provided by Dipeptide, Tripeptide, and Tetrapeptide Ligands. *J. Phys. Chem. A* **2007**, *111*, 11562−11571.
(69) Verkerk, U. H.; Zhao, J. F.; Saminathan, I. S.; Lau, J. K. C.; Oomens, J.; Hopkinson, A. C.; Siu, K. W. M. Infrared Multiple-Photon Dissociation Spectroscopy of Tripositive Ions: Lanthanum-Tryptophan Complexes. *Inorg. Chem.* **2012**, *51*, 4707−4710.